



HAL
open science

The Tail of the Striatum: From Anatomy to Connectivity and Function

Emmanuel Valjent, Giuseppe Gangarossa

► **To cite this version:**

Emmanuel Valjent, Giuseppe Gangarossa. The Tail of the Striatum: From Anatomy to Connectivity and Function. Trends in Neurosciences, 2021, 44 (3), pp.203-214. 10.1016/j.tins.2020.10.016 . hal-03052590

HAL Id: hal-03052590

<https://hal.science/hal-03052590v1>

Submitted on 10 Mar 2023

HAL is a multi-disciplinary open access archive for the deposit and dissemination of scientific research documents, whether they are published or not. The documents may come from teaching and research institutions in France or abroad, or from public or private research centers.

L'archive ouverte pluridisciplinaire **HAL**, est destinée au dépôt et à la diffusion de documents scientifiques de niveau recherche, publiés ou non, émanant des établissements d'enseignement et de recherche français ou étrangers, des laboratoires publics ou privés.



Distributed under a Creative Commons Attribution - NonCommercial 4.0 International License

1 **The Tail of the Striatum: from anatomy to connectivity and function**

2

3 Emmanuel Valjent¹ and Giuseppe Gangarossa²

4

5 ¹IGF, University of Montpellier, CNRS, INSERM, Montpellier, France

6 ²Université de Paris, BFA, UMR 8251, CNRS, F-75013 Paris, France

7

8

9 Correspondence to: giuseppe.gangarossa@u-paris.fr (GG, [@PeppeGanga](#)) and
10 emmanuel.valjent@igf.cnrs.fr (EV)

11

12

13

14

15 Keywords: striatal heterogeneity; dopamine receptors; reward and aversive behaviors;
16 psychostimulants; striatal projection neurons

17 **Abstract**

18 The dorsal striatum, the largest subcortical structure of the basal ganglia, is critical in
19 controlling motor, procedural and reinforcement-based behaviors. Although in mammals the
20 striatum extends widely along the rostro-caudal axis, current knowledge and derived theories
21 about its anatomo-functional organization largely rely on results obtained from studies of its
22 rostral sectors, leading to potentially oversimplified working models of the striatum as a
23 whole. Recent findings indicate that the extreme caudal part of the striatum, also referred to as
24 the tail of striatum (TS), represents an additional functional domain. Here, we provide an
25 overview of past and recent studies revealing that the TS displays a heterogeneous cell-type-
26 specific organization and a unique input-output connectivity which poises the TS as an
27 integrator of sensory processing.

28 **The forgotten territories of the striatum**

29 The dorsal striatum is the main gateway of the basal ganglia, a group of subcortical nuclei
30 which ensures motor control, action selection, decision making, as well as procedural and
31 reinforcement-based learning [1–3]. In mammals, the striatum is primarily composed of
32 GABAergic striatal projection neurons (SPNs) onto which converge glutamatergic projections
33 from the entire cerebral cortex, thalamus and limbic regions including the hippocampus and
34 amygdala. The multimodal signals conveyed by corticostriatal and thalamostriatal inputs are
35 detected and integrated by SPNs [4]. The computed relevant information is in turn relayed to
36 the output structures of the basal ganglia, thereby allowing the selection and execution of
37 optimized motor sequences [5–8]. These filtering properties are also tightly modulated by
38 monoaminergic signals conveyed by dopaminergic and serotonergic projections originating
39 from the midbrain dopamine (DA) neurons and dorsal raphe nucleus, respectively [9,10].

40 Despite decades of research, the anatomo-functional organization of the striatum is far
41 from being fully understood. This quest has been largely hampered by the lack of anatomical
42 markers allowing the clear delimitation of territorial boundaries. To date, three major
43 functional domains, dynamically interacting with each other, have been delineated according
44 to the topographic organization of glutamatergic and monoaminergic projections: *i*) the
45 sensorimotor domain comprising the dorsolateral striatum and involved in habit formations,
46 *ii*) the associative domain corresponding to the dorsomedial striatum and important for
47 driving goal-directed behavior, and *iii*) the limbic domain which mediates motivational and
48 affective functions and extend to the ventral striatum [11–15]. Our current understanding of
49 the anatomo-functional organization of striatal circuits has undoubtedly benefited from the
50 delineation of these domains. However, these distinct territories have been defined based on
51 differences spanning across the mediolateral and dorsoventral axes of the rostral striatum. The
52 absence of additional functional domains is somehow surprising since the striatum extends

53 along the rostro-caudal axis in mammalian brains. Interestingly, recent studies have started
54 providing new insights into the organization of striatal circuits, supporting the existence of at
55 least a fourth striatal functional domain located in the extreme caudal part of the dorsal
56 striatum, also known as the tail of striatum (TS) (**Figure 1**). Here, we summarize key
57 evidence revealing the peculiar anatomo-functional organization of the TS as characterized,
58 among other features, by the non-random spatial distribution of SPNs-expressing dopamine
59 D1 and D2 receptors (D1R-SPNs and D2R-SPNs). We also discuss the high responsiveness of
60 signaling pathways in TS SPNs to psychostimulants. Finally, we review recent findings
61 supporting the role of the TS in guiding appetitive and aversive behaviors relying on the
62 processing of visual and auditory information.

63

64 **Characterizing the TS by its connectivity**

65 *Excitatory afferents*

66 The term “tail of the striatum” (TS) was early attributed to the rat striatal domain receiving
67 cortical projections from the visual cortex [16]. Subsequently, detailed characterization of
68 rodents’ cortical afferents projecting to the TS identified the sensorimotor, visual, and
69 auditory cortices as the main sources of TS-projecting neurons [17]. These pioneering
70 observations have been recently confirmed, and further extended, by large-scale projectome
71 studies, whose advanced analyses have precisely redefined the corticostriatal connectivity
72 throughout the rostro-caudal extension of the striatum, including the TS [18–22]. Additional
73 inputs arising from the agranular/granular/dysgranular insular cortices, frontal and temporal
74 association cortices, motor cortex and ecto/peri/entorhinal cortices have been recently
75 described, thus refining the corticostriatal projections map within the TS [18–21] (**Figure 1**).
76 Beyond corticostriatal afferents, inputs from distinct subcortical structures including the
77 amygdala, subiculum, claustrum and endopiriform nucleus also converge into the TS,

78 suggesting that multisensory processing is likely to occur in the TS [19,20] (**Figure 1**). The
79 degree of convergence into the TS of the aforementioned inputs is however not shared by all
80 mammals. For instance, the caudate tail and posterolateral putamen in cats or macaque
81 monkeys receive almost exclusively excitatory inputs from the visual cortex [23,24]. These
82 observations suggest that the anatomic-functional organization of corticostriatal projections
83 tends to be more segregated throughout the rostro-caudal axis in species in which the dorsal
84 striatum has anatomically demarcated caudate and putamen nuclei.

85 Although thalamostriatal afferents are evolutionary more ancient than corticostriatal
86 projections, the role of this excitatory network has been for a long time overlooked [25,26].
87 The analysis of large tracing datasets has recently provided a detailed map of thalamostriatal
88 afferents innervating the rodents' dorsal striatum, including the TS [19,20]. Thus, thalamic
89 nuclei, including the lateral and medial geniculate nuclei, the lateral and ventral posterior
90 nucleus, the parafascicular and posterior intralaminar nuclei, represent the principal sources of
91 thalamic inputs into the TS [19,20,27,28] (**Figure 1**). Interestingly, a similar pattern of
92 connectivity has also been described in the brain of cats, tree shrews and non-human primates
93 [29–32].

94

95 *Monoaminergic afferents*

96 The functional domains of the striatum receive massive projections from three segregated
97 clusters of DA neurons located in the midbrain [33]. The ones arising from the substantia
98 nigra *pars compacta* (SNc, or A9 group) primarily project to the dorsal striatum, whereas
99 those originating from the retrorubral field (RrF, or A8 group) and the ventral tegmental area
100 (VTA, or A10 group) mainly innervate the ventral striatum [34]. Within these clusters,
101 molecularly-defined SNc and VTA DA neurons displayed biased projections along the
102 rostrocaudal, mediolateral and dorsoventral axes of the DS [33]. Thus, while DA neurons

103 located to the ventral and dorsal tier of the SNc project massively to the lateral and the
104 ventromedial part of the rostral and intermediate DS, respectively, TS-projecting DA neurons
105 arise almost exclusively from the substantia nigra *pars lateralis* (SNpl) [33,35–37]. Similarly,
106 DA neurons projecting to the tail of the caudate nucleus (CDt) in cats or monkeys are
107 preferentially located in SNpl, thus revealing that the topographic organization of DA
108 innervation is highly conserved in mammal brains [38,39] (**Figure 1**). Advances in the
109 development of cell-type-specific trans-synaptic tracing methods have allowed to establish a
110 comprehensive cartography of the connectivity of TS-projecting DA neurons [36].
111 Interestingly, unlike DA neurons innervating rostral sectors of the dorsal striatum, TS-
112 projecting DA neurons receive a specific set of monosynaptic inputs from the globus pallidus,
113 zona incerta, parasubthalamic and subthalamic nuclei, entopeduncular nucleus and SNr [36].
114 The peculiarity of TS-projecting DA neurons is also supported by their unique molecular
115 signature characterized by the co-expression of the vesicular glutamate transporter 2
116 (VGLUT2) and the lack of dopamine D2 autoreceptors [33,35,37,40]. These neurochemical
117 features reveal that TS-projecting DA neurons *i*) may co-release DA and glutamate and *ii*)
118 may use other mechanisms than D2R to control the timing and the amount of DA released
119 from presynaptic terminals. Although less characterized, serotonergic (5-HT) innervation
120 from the dorsal raphe nucleus (DRN) has also been described in the TS of rodents as well as
121 in the caudate nucleus of monkeys, thus constituting a second important source of
122 neuromodulation [20,41] (**Figure 1**).

123

124 *TS efferents*

125 TS-output neurons, which consist of SPNs, are segregated into two distinct populations
126 projecting either to the caudal part of the external globus pallidus (GPe) (iSPNs) or to the
127 Ep/GPi and SNr (dSPNs) (**Figure 1**). In the latter, striatal projections arising from the TS are

128 topographically organized as longitudinal lamina located in the ventral SNr extending from its
129 medial and to its lateral part and comprising the *pars lateralis* [17]. Cell-type-specific tracing
130 tools have been again determinant in defining the circuits controlled by TS SPNs. Thus, TS-
131 output neurons establish monosynaptic contacts with DA neurons located in the SNpl [42] as
132 well as with GABAergic neurons of the lateral SNr [43]. This latter population, which
133 projects to motor thalamic nuclei innervating the M1 and M2 motor cortices, supports the
134 existence of open motor loops that might explain how striatal sub-regions involved in sensory
135 processing modulate and tune motor control outputs [43]. Importantly, anatomical and
136 electrophysiological investigations in the primate CDt have indicated a similar efferent
137 organization for CDt-output dSPNs and iSPNs [44–46], even though a small percentage of
138 traced CDt SPNs (~15%) projected to both caudal SNr and GPe [45].

139

140 **Delineation of the rodent's TS by its unique cellular architecture**

141 The quest for anatomical markers allowing the delimitation of the TS has only begun. The use
142 of transgenic mice expressing reporters (fluorescent proteins, epitope-tagged proteins, Cre
143 recombinase) driven by specific promoters enables the delimitation of TS domains (**Table 1**).
144 Based on the differential distribution of SPNs expressing either D1R or D2R or both, our
145 group has recently proposed the existence of at least three TS domains: *i*) a D2R/A2aR-SPNs-
146 lacking domain, *ii*) a D1R- and D2R/A2aR-SPNs-intermingled domain and *iii*) a D1R/D2R-
147 SPNs-coexpressing domain [47].

148

149 *The D2R/A2aR-SPNs-lacking domain*

150 In the course of our attempt of characterizing the spatial distribution of D1R- and D2R-SPNs
151 throughout the rostro-caudal axis of the striatum, we have uncovered in the TS the existence
152 of a longitudinal stripe adjacent to the GPe comprising D1R-expressing SPNs exclusively

153 [35,47]. The absence of D2R/A2aR-SPNs was further supported by the lack of expression of
154 specific markers of this SPN population including D2R, A2aR, enkephalin, Gpr6 and 5'-
155 nucleotidase [48–51]. To date, this represents the best cellular hallmark of this first TS
156 domain which most likely corresponds to the medial part of the TS tri-laminar zone recently
157 described [47,50] (**Figure 2**). The D2R/A2aR-SPNs-lacking domain is also identifiable by a
158 dense plexus of fibers immunoreactive for substance P [35,50], reminiscent of the one
159 described in the “marginal division” (MrD) [52]. However, the lack of μ opioid receptor
160 (MOR) and enkephalin immunoreactivities in D2R/A2aR-SPNs-lacking domain compared to
161 the MrD indicates that they may not be one and the same caudal domain [35,50,52].

162 Local GABA- and ACh-releasing interneurons, which represent ~5% of striatal neurons,
163 play a fundamental role in governing the activity and functions of the striatum [53–55].
164 Beside the peculiar spatial arrangement of D1R-SPNs and D2R-SPNs, a differential
165 distribution of NOS- and ChAT-containing interneurons has been observed in the mouse TS
166 [50]. This cellular feature is of interest, since striatal ChAT interneurons are generally
167 characterized by the co-expression of D2R [56]. In fact, whereas ~94% of ChAT interneurons
168 co-expressed GFP in the dorsal striatum of *Drd2*-eGFP mice, such percentage dropped down
169 to ~17% in the D2R/A2aR-SPNs lacking domain of the TS [35], thereby highlighting a
170 further cellular heterogeneity along the rostro-caudal striatal axis. Importantly, via local cell-
171 to-cell communication, D2R-SPNs and ChAT interneurons are known to modulate the
172 activity of D1R-SPNs [57–62]. Recently, by implementing experimental data with *in silico*
173 modeling, it has been estimated that D2R-SPNs show higher probability to form synaptic
174 contacts with SPNs (both D1R-SPNs and D2R-SPNs) than D1R-SPNs [61,63,64].
175 Interestingly, the virtual absence of D2R-SPNs and the low percentage of ChAT/D2R-
176 positive interneurons in the TS D2R/A2aR-SPNs lacking domain indicate that D1R-SPNs

177 may possess unique physiological properties (reduced inhibitory drive) that indeed require
178 further mechanistic and functional investigations.

179

180 *The D1R- and D2R/A2aR-SPNs-intermingled domain*

181 Adjacent to the D2R/A2aR-SPNs-lacking domain, we have identified a D1R- and D2R/A2aR-
182 SPNs-intermingled domain which extends laterally throughout the dorso-ventral axis of the
183 TS [47]. This domain has been further subdivided into two zones corresponding to the
184 intermediate and lateral parts of the tri-laminar zone, respectively [50]. Despite their recent
185 description, up to ten markers can be used to delineate these two zones (**Figure 2, Table 1**).
186 The intermediate zone displays an ovoid shape easily identifiable by the low expression of
187 TH- and DAT-containing fibers [35,47,50]. This zone is also characterized by low levels of
188 D1R and high expression of D2R/A2aR consistent with reduced number of D1R-SPNs
189 compared to D2R/A2aR-SPNs [47,50]. The lateral zone is delineated by an intense
190 enkephalin labeling and a high PKC γ expression [50] (**Figure 2**). Interestingly, corticostriatal
191 sensory projections innervating these two zones are highly segregated. Indeed, the
192 intermediate zone receives excitatory inputs from the auditory cortex, whereas the lateral zone
193 is preferentially innervated by the agranular insular cortex [21]. All these anatomical features,
194 which are highly conserved across the *Muridae* family (mouse, rat, gerbil), suggest that this
195 topographic organization may have functional consequences by compartmentalizing the
196 sensory-related processes integrated and relayed by the TS [47].

197

198 *D1R/D2R-SPNs-coexpressing domain*

199 The third TS domain lies between the central amygdala (CeA), and the D1R- and D2R/A2aR-
200 SPNs-intermingled domain [47]. This domain is characterized by a proportion of D1R/D2R-
201 coexpressing SPNs (~33%, [47]) much higher than that reported in the dorsal and ventral

202 regions of the rostral striatum, thus constituting one of its main anatomical features
203 [35,47,65–69]. This domain most likely corresponds to the amygdalo-striatal transition area
204 (AST), which processes, together with the adjacent CeA, emotionally relevant information
205 **(Box 1)**.

206

207 **Hyper-responsiveness of TS neurons to psychostimulants**

208 Over the past decades, the analysis of DA-evoked molecular signaling events, such as the
209 post-translational modifications (phosphorylation) of ERK, histone H3, and ribosomal protein
210 S6 (rpS6), have been commonly used as molecular readouts for monitoring the activation of
211 SPNs in response to appetitive, aversive and pharmacological stimuli [70]. This approach has
212 provided the first insights into the differential functions of the TS domains.

213 The activation of SPNs in the TS was first described in response to systemic administration
214 of the D1R agonist SKF81297 [71]. Topographic and cell-type-specific analyses indicated
215 that ERK, histone H3, and rpS6 phosphorylations were specifically enhanced in D1R-SPNs
216 located in TS zones processing visual and auditory information [71]. According to the
217 recently proposed delineation of TS territories, the phosphorylation of ERK was restricted to
218 the D2/A2aR-SPNs-lacking domain (medial zone) and the lateral and dorsal parts of the D1R-
219 and D2R/A2aR-SPNs-intermingled domain [47]. Similar patterns of DA-dependent ERK,
220 histone H3 and rpS6 phosphorylation were observed after acute administration of d-
221 amphetamine, methamphetamine, cocaine, methylphenidate, 3,4-
222 methylenedioxymethamphetamine (MDMA) or GBR12783, a selective inhibitor of DA
223 reuptake [47,72] **(Figure 3)**. These DA-dependent signaling events, which occurred
224 selectively in D1R-SPNs, depend on the stimulation/activation of D1R [47,72]. Interestingly,
225 ERK activation in the TS appears to be selective for psychostimulants since other classes of
226 drugs, such as hallucinogens (2,5-dimethoxy-4-iodoamphetamine, phencyclidine,

227 dizocilpine), antidepressants (desipramine, fluoxetine), antipsychotics (haloperidol,
228 raclopride) or mood stabilizers (lithium), failed to trigger ERK activation [47]. Further studies
229 are needed to determine whether this pattern of ERK activation is specific to psychostimulants
230 or shared by other classes of drugs of abuse as it is the case in the shell of the nucleus
231 accumbens and the extended amygdala [73].

232 Although D1R-mediated ERK, histone H3, and rpS6 phosphorylations require the
233 activation of the cAMP/PKA pathway in both the rostral parts of the dorsal striatum and the
234 TS, recent work indicates that the underlying molecular mechanisms might be different
235 [47,72,74]. Several explanations may account for the potent ERK activation in the D1R-SPNs
236 of the TS D2R/A2aR-SPNs-lacking domain compared to those of the antero-dorsal striatum
237 [47]. Indeed, the absence of the tonic inhibition on ERK phosphorylation mediated by the
238 collateral inhibition of D2R-SPNs onto D1R-SPNs of the medial zone could be one of them.
239 In fact, the D1R-dependent ERK phosphorylation in the antero-dorsal striatum is enhanced in
240 mice lacking D2R in D2R/A2aR-SPNs [75]. Moreover, evidence suggest that the inactivation
241 of the cAMP/PKA signaling normally achieved by PDE1b, PDE10A and PDE4, three SPNs-
242 enriched phosphodiesterases (PDEs) isoforms [76], might not be optimal. Indeed, the lack of
243 PDEs activities in D1R-SPNs of the medial zone certainly account for the rapid and sustained
244 cAMP-dependent phosphorylation of ERK, histone H3 and rpS6 observed in the TS compared
245 to the rostral sectors of the dorsal striatum [35,47,71] (**Figure 3**). Future studies are needed to
246 determine whether D1R-SPNs of the TS D2R/A2aR-SPNs-lacking domain display unique
247 molecular, physiological and functional features (**Figure 3, Box 2**).

248

249 **The TS as an integrator of sensory processing**

250 Although the ability of TS SPNs to respond to a broad range of auditory stimulations has been
251 established for decades [77], only recently the role of the TS in processing auditory

252 information has regained interest. Specifically, recent studies have demonstrated that the
253 acquisition of a sound-driven discrimination task is accompanied by an enhanced auditory
254 corticostriatal plasticity [78,79]. Consequently, inhibition of the auditory corticostriatal
255 excitatory inputs, which tune information for striatum-dependent sound representations,
256 impaired behavioral performance in an auditory frequency discrimination task [27]. It should
257 be noted here that recently identified corticostriatal long-range inhibitory circuits might also
258 contribute to the regulation of auditory processing [80,81]. Similarly, altered responses have
259 been described following the inactivation of thalamostriatal inputs onto TS SPNs, thereby
260 suggesting that both excitatory inputs are necessary to orchestrate auditory decision-making
261 [27]. In addition, inactivation of TS D1R-SPNs impaired sound discrimination and the
262 execution of behavioral tasks requiring auditory decisions [82]. Collectively, these studies
263 support the key role of TS SPNs in integrating auditory sensory information with reward-
264 associated signals to adjust and drive appropriate behavior [83]. A striking observation is that
265 a transient auditory deprivation during development yields to persistent alterations in TS
266 SPNs, thereby suggesting that the acquisition of their auditory-tuning properties might be
267 permanently established during a brief developmental critical period [22]. This latter
268 observation might explain the origin of striatal dysfunctions observed in sensory disorders
269 associated with auditory processing [84,85]. Future studies will be essential in determining
270 whether similar developmental mechanisms regulate the maturation of TS SPNs involved in
271 visual information processing.

272 Reinforcement learning driven by visual and auditory stimuli relies in part on the ability of
273 midbrain DA neurons to encode reward prediction error (RPE), salience and novelty [86–89].
274 Recent work indicates that TS-projecting DA neurons are functionally distinct from DA
275 neurons innervating the dorsal and ventral sectors of the rostral striatum. Photometric Ca^{2+}
276 recordings of DA axons have been determinant in demonstrating that TS-projecting DA

277 neurons are not only excited in response to novel cues but also by a variety of external
278 sensory stimuli perceived as rewarding, aversive or neutral [90,91]. Their ability to convey
279 general salient signals largely contribute to process reinforcement signals that promote
280 avoidance of threatening stimuli [91]. Further studies are needed to precisely define whether
281 reinforcement learning based on external threats engages distinct TS circuits depending on the
282 nature and the anatomical sources of sensory stimuli (auditory, visual, somatosensory).

283 Some similarities may exist between the function of TS-projecting DA neurons in rodents
284 and those projecting to the tail of the caudate (CDt) in primates. Indeed, midbrain DA neurons
285 located in the dorsolateral part of the SNc are excited by both rewarding and aversive stimuli
286 [88]. Importantly, these neurons, which also respond to salient visual stimuli, are thought to
287 facilitate long-term memory of reward values of visual objects contributing to automatic and
288 habitual saccades [92]. Importantly, at least two functionally distinct types of DA neurons
289 have been highlighted in the primate SNc: the rostro-medial “update-type DA neurons”
290 which, by mainly projecting to the caudate head (CDh), respond to unpredicted changes, and
291 the CDt-projecting rostro-lateral “sustain-type DA neurons” which encode habitual behaviors
292 [92]. Such functions might support a role of SPNs of the caudate tail in reward-driven
293 visuomotor processing [93–95]. In line with the visual-related functions processed by the
294 primate CDt, lesions of this striatal caudal region elicited an impairment of visual habit
295 formation while sparing visual recognition memory [96]. In addition, neurons of the primate
296 CDt, in opposition to the CDh, have been shown to selectively control automatic saccades-
297 guided behavior when values of visual objects were more stable than flexible, the latter being
298 dependent on the CDh [97]. Recently, taking advantage of optogenetic strategies, a role for
299 CDt D1R-SPNs and D2R-SPNs has emerged as facilitators or suppressors of values-guided
300 saccades, respectively [44,46]. However, whether sensory-related visual and/or auditory

301 stimuli are processed similarly in the TS/CDt of other species (i.e. human) remain to be fully
302 established.

303

304 **Concluding remarks**

305 Parsing how the dorsal striatum is functionally organized has been largely hampered by the
306 lack of anatomical markers allowing the clear delimitation of territorial boundaries. Current
307 knowledge on striatal functions and dysfunctions is mainly built upon evidence obtained on
308 rostral sectors of the striatum. However, recent data emerging from large-scale projectome
309 studies have enabled refining the anatomo-functional organization of the dorsal striatum, thus
310 suggesting that the TS may constitute a fourth striatal functional domain. Beyond a unique
311 corticostriatal, thalamostriatal and nigrostriatal connectivity, recent findings indicate that,
312 unlike in most rostral sectors of the dorsal striatum, segregated D1R- and D2R-SPNs are not
313 randomly distributed in the rodents' TS. Future studies are needed to determine whether this
314 key anatomical feature exists in other mammal species, including in non-human and human
315 primate brains.

316 The existence of anatomically distinct TS domains raises questions about their functions.
317 As mentioned above, the TS participates in encoding visual and auditory stimuli, thus
318 representing a functional hub to allow sensory-associated reward, motor, aversive and
319 decision-making functional outputs. However, how the TS territories and their cell-type
320 components control such functional outputs remains to be established. The recent
321 development of advanced methodologies combining rabies-mediated trans-synaptic tracing
322 and Cre-based cell-type-specific targeting [98] will be valuable to precisely map
323 monosynaptic inputs onto D1R- and D2-SPNs located in the distinct TS domains. Such
324 anatomical characterization will be necessary to understand whether sensory (mainly visual
325 and auditory) information is processed independently by each TS domain. Eventually, single-

326 cell gene expression profiling will enable defining whether molecular heterogeneity exists
327 amongst TS SPNs that might help to better understand how information is computed in the TS
328 to guide behaviors.

329 **Box 1: The amygdalo-striatal transition area (AST)**

330 Despite its description more than four decades ago, the anatomo-functional organization of
331 the amygdalo-striatal transition area (AST) in rodents and primates remains largely enigmatic
332 [99–102]. Located between the TS and the central nucleus of the amygdala, adjacent to the
333 caudal globus pallidus, the AST receives massive projections from visual and auditory
334 thalamic centers as well as from the insula and amygdala nuclei [100,103–105]. The
335 connectivity and cellular composition of the AST closely resembles those described for the
336 dorsal striatum. Indeed, AST-output neurons segregate and project to the substantia nigra *pars*
337 *lateralis* and caudoventral globus pallidus [100,106,107]. At the cellular and molecular levels,
338 AST-output neurons comprise D1R-, D2R- and D1R/D2R-SPNs distributed in a random and
339 equal proportion [47]. The AST is characterized by intense calretinin and angiotensin II
340 immunoreactivities, two histological features shared with the extended amygdala [100,105].
341 Although early studies have suggested a role in the regulation emotional responses [106,108],
342 future studies are required to determine whether salient events are integrated and processed at
343 the level of the AST, and if so, how AST-output neurons contribute to guide motivated
344 behaviors.

345 **Box 2: Molecular and cellular heterogeneity within TS domains**

346 Recent methodological advances in gene expression profiling have unveiled an unexpected
347 molecular heterogeneity among D1R- and D2R-SPNs throughout the dorso-ventral axis of the
348 anterior striatum [56,109,110]. This molecular diversity appears to follow a specific spatial
349 organization as illustrated by recent studies establishing spatio-molecular maps of SPNs in
350 patch, matrix and exopatch compartments [111,112]. Interestingly, emerging evidence points
351 to an additional level of molecular heterogeneity among SPNs throughout the striatal rostro-
352 caudal axis, notably at the level of the TS. Indeed, the absence and/or inefficacy of SPNs-
353 enriched PDEs or phosphatases in D1R-SPNs of the D2R/A2aR-SPNs-lacking TS domain
354 may account for the sustained and enhanced phosphorylation events dependent on cyclic
355 nucleotide signaling [47]. The molecular heterogeneity is not restricted to SPNs since only
356 ~17% of the cholinergic interneurons located in the D2R/A2aR-SPNs-lacking domain express
357 D2R [35]. This observation suggest that the diversity of striatal cholinergic interneurons is not
358 restricted to the dorsoventral axis but also exist throughout the rostro-caudal axis [56,113].
359 Similar diversity may certainly exist in other striatal interneurons subtypes [114]. Finally, the
360 use of barcoded anatomy resolved by sequencing (BARseq) [115] may provide important
361 insights into the organizing principles underlying the anatomo-functional organization of TS
362 circuits.

363 **Acknowledgments**

364 We thank Denis Hervé and Jean-Antoine Girault for critical reading of the manuscript and for
365 their insightful comments. This work was supported by Inserm, Fondation pour la Recherche
366 Médicale (DEQ20160334919) (E.V.), La Marato de TV3 Fundacio (#113-2016) (E.V.), and
367 Agence National de la Recherche (EPITRACES, ANR-16-CE16-0018; DOPAFEAR, ANR-
368 16-CE16-0006) (E.V.), Université de Paris, Nutricia Research Foundation (G.G.), Allen
369 Foundation Inc. (G.G.), Fyssen Foundation (G.G.).

370 **References**

- 371 1 Hikida, T. *et al.* (2010) Distinct roles of synaptic transmission in direct and indirect
372 striatal pathways to reward and aversive behavior. *Neuron* 66, 896–907
- 373 2 Kravitz, A.V. and Kreitzer, A.C. (2012) Striatal mechanisms underlying movement,
374 reinforcement, and punishment. *Physiology (Bethesda)* 27, 167–177
- 375 3 Lee, D. *et al.* (2012) Neural basis of reinforcement learning and decision making.
376 *Annu. Rev. Neurosci.* 35, 287–308
- 377 4 Wall, N.R. *et al.* (2013) Differential innervation of direct- and indirect-pathway striatal
378 projection neurons. *Neuron* 79, 347–360
- 379 5 Peak, J. *et al.* (2019) From learning to action: the integration of dorsal striatal input
380 and output pathways in instrumental conditioning. *Eur. J. Neurosci.* 49, 658–671
- 381 6 Hidalgo-Balbuena, A.E. *et al.* (2019) Sensory representations in the striatum provide a
382 temporal reference for learning and executing motor habits. *Nat Commun* 10, 4074
- 383 7 Jin, X. and Costa, R.M. (2010) Start/stop signals emerge in nigrostriatal circuits during
384 sequence learning. *Nature* 466, 457–462
- 385 8 Jin, X. *et al.* (2014) Basal ganglia subcircuits distinctively encode the parsing and
386 concatenation of action sequences. *Nat. Neurosci.* 17, 423–430
- 387 9 Cavaccini, A. *et al.* (2018) Serotonergic Signaling Controls Input-Specific Synaptic
388 Plasticity at Striatal Circuits. *Neuron* 98, 801-816.e7
- 389 10 Lerner, T.N. *et al.* (2015) Intact-Brain Analyses Reveal Distinct Information Carried
390 by SNc Dopamine Subcircuits. *Cell* 162, 635–647
- 391 11 Balleine, B.W. and O’Doherty, J.P. (2010) Human and rodent homologues in action
392 control: corticostriatal determinants of goal-directed and habitual action.
393 *Neuropsychopharmacology* 35, 48–69
- 394 12 Thorn, C.A. *et al.* (2010) Differential dynamics of activity changes in dorsolateral and
395 dorsomedial striatal loops during learning. *Neuron* 66, 781–795
- 396 13 Voorn, P. *et al.* (2004) Putting a spin on the dorsal-ventral divide of the striatum.
397 *Trends Neurosci.* 27, 468–474
- 398 14 Gremel, C.M. and Costa, R.M. (2013) Orbitofrontal and striatal circuits dynamically
399 encode the shift between goal-directed and habitual actions. *Nat Commun* 4, 2264
- 400 15 Floresco, S.B. (2015) The nucleus accumbens: an interface between cognition,
401 emotion, and action. *Annu Rev Psychol* 66, 25–52
- 402 16 Donoghue, J.P. and Herkenham, M. (1986) Neostriatal projections from individual
403 cortical fields conform to histochemically distinct striatal compartments in the rat. *Brain Res.*
404 365, 397–403
- 405 17 Deniau, J.M. *et al.* (1996) The lamellar organization of the rat substantia nigra pars
406 reticulata: segregated patterns of striatal afferents and relationship to the topography of

407 corticostriatal projections. *Neuroscience* 73, 761–781

408 18 Hintiryan, H. *et al.* (2016) The mouse cortico-striatal projectome. *Nat. Neurosci.* 19,
409 1100–1114

410 19 Hunnicutt, B.J. *et al.* (2016) A comprehensive excitatory input map of the striatum
411 reveals novel functional organization. *Elife* 5,

412 20 Jiang, H. and Kim, H.F. (2018) Anatomical Inputs From the Sensory and Value
413 Structures to the Tail of the Rat Striatum. *Front Neuroanat* 12, 30

414 21 Miyamoto, Y. *et al.* (2018) Striosome-based map of the mouse striatum that is
415 conformable to both cortical afferent topography and uneven distributions of dopamine D1
416 and D2 receptor-expressing cells. *Brain Struct Funct* 223, 4275–4291

417 22 Mowery, T.M. *et al.* (2017) The Sensory Striatum Is Permanently Impaired by
418 Transient Developmental Deprivation. *Cell Rep* 19, 2462–2468

419 23 Updyke, B.V. (1993) Organization of visual corticostriatal projections in the cat, with
420 observations on visual projections to claustrum and amygdala. *J. Comp. Neurol.* 327, 159–193

421 24 Seger, C.A. (2013) The visual corticostriatal loop through the tail of the caudate:
422 circuitry and function. *Front Syst Neurosci* 7, 104

423 25 Smith, Y. *et al.* (2004) The thalamostriatal system: a highly specific network of the
424 basal ganglia circuitry. *Trends Neurosci.* 27, 520–527

425 26 Reiner, A. *et al.* (2005) Organization and evolution of the avian forebrain. *Anat Rec A*
426 *Discov Mol Cell Evol Biol* 287, 1080–1102

427 27 Chen, L. *et al.* (2019) Medial geniculate body and primary auditory cortex
428 differentially contribute to striatal sound representations. *Nat Commun* 10, 418

429 28 Ponvert, N.D. and Jaramillo, S. (2019) Auditory Thalamostriatal and Corticostriatal
430 Pathways Convey Complementary Information about Sound Features. *J. Neurosci.* 39, 271–
431 280

432 29 Beckstead, R.M. (1984) A projection to the striatum from the medial subdivision of
433 the posterior group of the thalamus in the cat. *Brain Res.* 300, 351–356

434 30 Day-Brown, J.D. *et al.* (2010) Pulvinar projections to the striatum and amygdala in the
435 tree shrew. *Front Neuroanat* 4, 143

436 31 Galvan, A. and Smith, Y. (2011) The primate thalamostriatal systems: Anatomical
437 organization, functional roles and possible involvement in Parkinson’s disease. *Basal Ganglia*
438 1, 179–189

439 32 Harting, J.K. *et al.* (2001) Striatal projections from the cat visual thalamus. *Eur. J.*
440 *Neurosci.* 14, 893–896

441 33 Poulin, J.-F. *et al.* (2020) Classification of Midbrain Dopamine Neurons Using Single-
442 Cell Gene Expression Profiling Approaches. *Trends Neurosci.* 43, 155–169

443 34 Roeper, J. (2013) Dissecting the diversity of midbrain dopamine neurons. *Trends*

444 *Neurosci.* 36, 336–342

445 35 Gangarossa, G. *et al.* (2013) Spatial distribution of D1R- and D2R-expressing
446 medium-sized spiny neurons differs along the rostro-caudal axis of the mouse dorsal striatum.
447 *Front Neural Circuits* 7, 124

448 36 Menegas, W. *et al.* (2015) Dopamine neurons projecting to the posterior striatum form
449 an anatomically distinct subclass. *Elife* 4, e10032

450 37 Poulin, J.-F. *et al.* (2018) Mapping projections of molecularly defined dopamine
451 neuron subtypes using intersectional genetic approaches. *Nat. Neurosci.* 21, 1260–1271

452 38 Hontanilla, B. *et al.* (1996) A topographic re-evaluation of the nigrostriatal projections
453 to the caudate nucleus in the cat with multiple retrograde tracers. *Neuroscience* 72, 485–503

454 39 Kim, H.F. *et al.* (2014) Separate groups of dopamine neurons innervate caudate head
455 and tail encoding flexible and stable value memories. *Front Neuroanat* 8, 120

456 40 Yamaguchi, T. *et al.* (2013) Glutamate neurons in the substantia nigra compacta and
457 retrorubral field. *Eur. J. Neurosci.* 38, 3602–3610

458 41 Griggs, W.S. *et al.* (2017) Flexible and Stable Value Coding Areas in Caudate Head
459 and Tail Receive Anatomically Distinct Cortical and Subcortical Inputs. *Front. Neuroanat.*
460 11,

461 42 Watabe-Uchida, M. *et al.* (2012) Whole-brain mapping of direct inputs to midbrain
462 dopamine neurons. *Neuron* 74, 858–873

463 43 Aoki, S. *et al.* (2019) An open cortico-basal ganglia loop allows limbic control over
464 motor output via the nigrothalamic pathway. *Elife* 8,

465 44 Amita, H. *et al.* (2020) Optogenetic manipulation of a value-coding pathway from the
466 primate caudate tail facilitates saccadic gaze shift. *Nat Commun* 11, 1876

467 45 Amita, H. *et al.* (2019) Neuronal connections of direct and indirect pathways for stable
468 value memory in caudal basal ganglia. *Eur. J. Neurosci.* 49, 712–725

469 46 Kim, H.F. *et al.* (2017) Indirect Pathway of Caudal Basal Ganglia for Rejection of
470 Valueless Visual Objects. *Neuron* 94, 920-930.e3

471 47 Gangarossa, G. *et al.* (2019) Contrasting patterns of ERK activation in the tail of the
472 striatum in response to aversive and rewarding signals. *J. Neurochem.* DOI:
473 10.1111/jnc.14804

474 48 Harris, J.A. *et al.* (2014) Anatomical characterization of Cre driver mice for neural
475 circuit mapping and manipulation. *Front Neural Circuits* 8, 76

476 49 Koshimizu, Y. *et al.* (2008) Paucity of enkephalin production in neostriatal striosomal
477 neurons: analysis with preproenkephalin-green fluorescent protein transgenic mice. *Eur. J.*
478 *Neurosci.* 28, 2053–2064

479 50 Miyamoto, Y. *et al.* (2019) Three divisions of the mouse caudal striatum differ in the
480 proportions of dopamine D1 and D2 receptor-expressing cells, distribution of dopaminergic
481 axons, and composition of cholinergic and GABAergic interneurons. *Brain Struct Funct* 224,

482 2703–2716

483 51 Schoen, S.W. and Graybiel, A.M. (1993) Species-specific patterns of glycoprotein
484 expression in the developing rodent caudoputamen: association of 5'-nucleotidase activity
485 with dopamine islands and striosomes in rat, but with extrastriosomal matrix in mouse. *J.*
486 *Comp. Neurol.* 333, 578–596

487 52 Shu, S.Y. *et al.* (2003) New component of the limbic system: Marginal division of the
488 neostriatum that links the limbic system to the basal nucleus of Meynert. *J. Neurosci. Res.* 71,
489 751–757

490 53 Fino, E. *et al.* (2018) Region-specific and state-dependent action of striatal
491 GABAergic interneurons. *Nat Commun* 9, 3339

492 54 Gritton, H.J. *et al.* (2019) Unique contributions of parvalbumin and cholinergic
493 interneurons in organizing striatal networks during movement. *Nat. Neurosci.* 22, 586–597

494 55 Zucca, S. *et al.* (2018) Pauses in cholinergic interneuron firing exert an inhibitory
495 control on striatal output in vivo. *Elife* 7,

496 56 Puighermanal, E. *et al.* (2020) Functional and molecular heterogeneity of D2R
497 neurons along dorsal ventral axis in the striatum. *Nat Commun* 11, 1957

498 57 Czubayko, U. and Plenz, D. (2002) Fast synaptic transmission between striatal spiny
499 projection neurons. *Proc. Natl. Acad. Sci. U.S.A.* 99, 15764–15769

500 58 English, D.F. *et al.* (2011) GABAergic circuits mediate the reinforcement-related
501 signals of striatal cholinergic interneurons. *Nat. Neurosci.* 15, 123–130

502 59 Koos, T. *et al.* (2004) Comparison of IPSCs evoked by spiny and fast-spiking neurons
503 in the neostriatum. *J. Neurosci.* 24, 7916–7922

504 60 Oldenburg, I.A. and Ding, J.B. (2011) Cholinergic modulation of synaptic integration
505 and dendritic excitability in the striatum. *Curr. Opin. Neurobiol.* 21, 425–432

506 61 Taverna, S. *et al.* (2008) Recurrent collateral connections of striatal medium spiny
507 neurons are disrupted in models of Parkinson's disease. *J. Neurosci.* 28, 5504–5512

508 62 Witten, I.B. *et al.* (2010) Cholinergic interneurons control local circuit activity and
509 cocaine conditioning. *Science* 330, 1677–1681

510 63 Hjorth, J.J.J. *et al.* (2020) The microcircuits of striatum in silico. *Proc. Natl. Acad. Sci.*
511 *U.S.A.* 117, 9554–9565

512 64 Planert, H. *et al.* (2010) Dynamics of synaptic transmission between fast-spiking
513 interneurons and striatal projection neurons of the direct and indirect pathways. *J. Neurosci.*
514 30, 3499–3507

515 65 Gangarossa, G. *et al.* (2013) Distribution and compartmental organization of
516 GABAergic medium-sized spiny neurons in the mouse nucleus accumbens. *Front Neural*
517 *Circuits* 7, 22

518 66 Gagnon, D. *et al.* (2017) Striatal Neurons Expressing D1 and D2 Receptors are
519 Morphologically Distinct and Differently Affected by Dopamine Denervation in Mice. *Sci*

520 *Rep* 7, 41432

521 67 Wei, X. *et al.* (2018) Dopamine D1 or D2 receptor-expressing neurons in the central
522 nervous system. *Addict Biol* 23, 569–584

523 68 Frederick, A.L. *et al.* (2015) Evidence against dopamine D1/D2 receptor heteromers.
524 *Mol. Psychiatry* 20, 1373–1385

525 69 Rico, A.J. *et al.* (2017) Neurochemical evidence supporting dopamine D1–D2 receptor
526 heteromers in the striatum of the long-tailed macaque: changes following dopaminergic
527 manipulation. *Brain Struct Funct* 222, 1767–1784

528 70 Valjent, E. *et al.* (2019) Dopamine signaling in the striatum. In *Advances in Protein*
529 *Chemistry and Structural Biology* Academic Press

530 71 Gangarossa, G. *et al.* (2013) Combinatorial topography and cell-type specific
531 regulation of the ERK pathway by dopaminergic agonists in the mouse striatum. *Brain Struct*
532 *Funct* 218, 405–419

533 72 Biever, A. *et al.* (2015) PKA-dependent phosphorylation of ribosomal protein S6 does
534 not correlate with translation efficiency in striatonigral and striatopallidal medium-sized spiny
535 neurons. *J. Neurosci.* 35, 4113–4130

536 73 Valjent, E. *et al.* (2004) Addictive and non-addictive drugs induce distinct and specific
537 patterns of ERK activation in mouse brain. *Eur. J. Neurosci.* 19, 1826–1836

538 74 Polito, M. *et al.* (2015) Selective Effects of PDE10A Inhibitors on Striatopallidal
539 Neurons Require Phosphatase Inhibition by DARPP-32. *eNeuro* 2,

540 75 Dobbs, L.K. *et al.* (2019) D1 receptor hypersensitivity in mice with low striatal D2
541 receptors facilitates select cocaine behaviors. *Neuropsychopharmacology* 44, 805–816

542 76 Nishi, A. *et al.* (2008) Distinct roles of PDE4 and PDE10A in the regulation of
543 cAMP/PKA signaling in the striatum. *J. Neurosci.* 28, 10460–10471

544 77 Bordi, F. and LeDoux, J. (1992) Sensory tuning beyond the sensory system: an initial
545 analysis of auditory response properties of neurons in the lateral amygdaloid nucleus and
546 overlying areas of the striatum. *J. Neurosci.* 12, 2493–2503

547 78 Znamenskiy, P. and Zador, A.M. (2013) Corticostriatal neurons in auditory cortex
548 drive decisions during auditory discrimination. *Nature* 497, 482–485

549 79 Xiong, Q. *et al.* (2015) Selective corticostriatal plasticity during acquisition of an
550 auditory discrimination task. *Nature* 521, 348–351

551 80 Rock, C. *et al.* (2016) An inhibitory corticostriatal pathway. *Elife* 5,

552 81 Bertero, A. *et al.* (2020) Auditory Long-Range Parvalbumin Cortico-Striatal Neurons.
553 *Front Neural Circuits* 14, 45

554 82 Guo, L. *et al.* (2018) Stable representation of sounds in the posterior striatum during
555 flexible auditory decisions. *Nat Commun* 9, 1534

556 83 Guo, L. *et al.* (2019) Choice-Selective Neurons in the Auditory Cortex and in Its

557 Striatal Target Encode Reward Expectation. *J. Neurosci.* 39, 3687–3697

558 84 Shepherd, G.M.G. (2013) Corticostriatal connectivity and its role in disease. *Nat. Rev.*
559 *Neurosci.* 14, 278–291

560 85 Lim, S.-J. *et al.* (2019) Role of the striatum in incidental learning of sound categories.
561 *Proc. Natl. Acad. Sci. U.S.A.* 116, 4671–4680

562 86 Cohen, J.Y. *et al.* (2012) Neuron-type-specific signals for reward and punishment in
563 the ventral tegmental area. *Nature* 482, 85–88

564 87 Glimcher, P.W. (2011) Understanding dopamine and reinforcement learning: the
565 dopamine reward prediction error hypothesis. *Proc. Natl. Acad. Sci. U.S.A.* 108 Suppl 3,
566 15647–15654

567 88 Matsumoto, M. and Hikosaka, O. (2009) Two types of dopamine neuron distinctly
568 convey positive and negative motivational signals. *Nature* 459, 837–841

569 89 Morrens, J. *et al.* (2020) Cue-Evoked Dopamine Promotes Conditioned Responding
570 during Learning. *Neuron* 106, 142–153.e7

571 90 Menegas, W. *et al.* (2017) Opposite initialization to novel cues in dopamine signaling
572 in ventral and posterior striatum in mice. *Elife* 6,

573 91 Menegas, W. *et al.* (2018) Dopamine neurons projecting to the posterior striatum
574 reinforce avoidance of threatening stimuli. *Nat. Neurosci.* 21, 1421–1430

575 92 Kim, H.F. *et al.* (2015) Dopamine Neurons Encoding Long-Term Memory of Object
576 Value for Habitual Behavior. *Cell* 163, 1165–1175

577 93 Yamamoto, S. *et al.* (2012) What and where information in the caudate tail guides
578 saccades to visual objects. *J. Neurosci.* 32, 11005–11016

579 94 Yamamoto, S. *et al.* (2013) Reward value-contingent changes of visual responses in
580 the primate caudate tail associated with a visuomotor skill. *J. Neurosci.* 33, 11227–11238

581 95 Hikosaka, O. *et al.* (2014) Basal ganglia circuits for reward value-guided behavior.
582 *Annu. Rev. Neurosci.* 37, 289–306

583 96 Fernandez-Ruiz, J. *et al.* (2001) Visual habit formation in monkeys with neurotoxic
584 lesions of the ventrocaudal neostriatum. *Proc. Natl. Acad. Sci. U.S.A.* 98, 4196–4201

585 97 Kim, H.F. and Hikosaka, O. (2013) Distinct basal ganglia circuits controlling
586 behaviors guided by flexible and stable values. *Neuron* 79, 1001–1010

587 98 Sjulson, L. *et al.* (2016) Cell-Specific Targeting of Genetically Encoded Tools for
588 Neuroscience. *Annu. Rev. Genet.* 50, 571–594

589 99 Alheid, G.F. *et al.* (1998) The neuronal organization of the supracapsular part of the
590 stria terminalis in the rat: the dorsal component of the extended amygdala. *Neuroscience* 84,
591 967–996

592 100 Shammah-Lagnado, S.J. *et al.* (1999) Afferent connections of the interstitial nucleus
593 of the posterior limb of the anterior commissure and adjacent amygdalostratial transition area

594 in the rat. *Neuroscience* 94, 1097–1123

595 101 Cho, Y.T. *et al.* (2013) Cortico-amygdala-striatal circuits are organized as hierarchical
596 subsystems through the primate amygdala. *J. Neurosci.* 33, 14017–14030

597 102 Fudge, J.L. and Tucker, T. (2009) Amygdala projections to central amygdaloid
598 nucleus subdivisions and transition zones in the primate. *Neuroscience* 159, 819–841

599 103 Turner, B.H. and Herkenham, M. (1991) Thalamoamygdaloid projections in the rat: a
600 test of the amygdala’s role in sensory processing. *J. Comp. Neurol.* 313, 295–325

601 104 Doron, N.N. and Ledoux, J.E. (1999) Organization of projections to the lateral
602 amygdala from auditory and visual areas of the thalamus in the rat. *J. Comp. Neurol.* 412,
603 383–409

604 105 Jolkkonen, E. *et al.* (2001) Interconnectivity between the amygdaloid complex and the
605 amygdalostriatal transition area: a PHA-L study in rat. *J. Comp. Neurol.* 431, 39–58

606 106 LeDoux, J.E. *et al.* (1990) The lateral amygdaloid nucleus: sensory interface of the
607 amygdala in fear conditioning. *J. Neurosci.* 10, 1062–1069

608 107 Shammah-Lagnado, S.J. *et al.* (1996) Efferent connections of the caudal part of the
609 globus pallidus in the rat. *J. Comp. Neurol.* 376, 489–507

610 108 Trogrlic, L. *et al.* (2011) Context fear learning specifically activates distinct
611 populations of neurons in amygdala and hypothalamus. *Learn. Mem.* 18, 678–687

612 109 Gokce, O. *et al.* (2016) Cellular Taxonomy of the Mouse Striatum as Revealed by
613 Single-Cell RNA-Seq. *Cell Rep* 16, 1126–1137

614 110 Saunders, A. *et al.* (2018) Molecular Diversity and Specializations among the Cells of
615 the Adult Mouse Brain. *Cell* 174, 1015-1030.e16

616 111 Märtin, A. *et al.* (2019) A Spatiomolecular Map of the Striatum. *Cell Rep* 29, 4320-
617 4333.e5

618 112 Stanley, G. *et al.* (2020) Continuous and Discrete Neuron Types of the Adult Murine
619 Striatum. *Neuron* 105, 688-699.e8

620 113 Virk, M.S. *et al.* (2016) Opposing roles for serotonin in cholinergic neurons of the
621 ventral and dorsal striatum. *Proc. Natl. Acad. Sci. U.S.A.* 113, 734–739

622 114 Muñoz-Manchado, A.B. *et al.* (2018) Diversity of Interneurons in the Dorsal Striatum
623 Revealed by Single-Cell RNA Sequencing and PatchSeq. *Cell Rep* 24, 2179-2190.e7

624 115 Chen, X. *et al.* (2019) High-Throughput Mapping of Long-Range Neuronal Projection
625 Using In Situ Sequencing. *Cell* 179, 772-786.e19

626 116 Franklin, K. and Paxinos, G., K. The Mouse Brain in Stereotaxic Coordinates, 3rd
627 Edn. . (2008), Elsevier

628 117 Gong, S. *et al.* (2003) A gene expression atlas of the central nervous system based on
629 bacterial artificial chromosomes. *Nature* 425, 917–925

630

631

632 **Figure legends**

633 **Figure 1: Delineating the tail of the striatum.**

634 (a) Coronal view of the tail of the striatum (TS) across different species. In rodents, the TS
635 consists of one entity, whereas in tree shrews, cats and non-human primates the TS consists of
636 the tail of the caudate nucleus (CDt) and the posterolateral putamen. (b) Schematic of rodents'
637 TS inputs. The TS receives excitatory afferents (in violet) from a broad range of cortical areas
638 throughout its rostro-caudal extension (from bregma -1.22 mm to -0.94 mm). This includes
639 the frontal association cortex (FrA), motor cortex (M1/2), somatosensory cortex (S1/2),
640 agranular, granular, dysgranular insular cortex (AI/GI/DI), visual cortex (Vis), auditory cortex
641 (Aud), ecto-/peri-/entorhinal cortex (Rhi) and temporal association cortex (Tem). The TS also
642 integrates thalamic inputs arising from the lateral and ventral posterior nuclei (LP and
643 VPM/VPL), medial and lateral geniculate nuclei (MG and LG), mediodorsal nucleus (MD),
644 parafascicular nucleus (PF), posterior intralaminar nucleus (PIL) and pulvinar nucleus. The
645 two main sources of monoaminergic regulation comprise dopaminergic (DA) neurons (in
646 orange) arising from the substantia nigra *pars lateralis* (SNpl) and serotonergic (5-HT) (in
647 turquoise) innervation from the dorsal raphe nucleus (DRN). (c) Schematic of rodents' TS
648 efferents. TS-output neurons are GABAergic SPNs that segregate into two distinct
649 populations projecting either to the caudal part of the external globus pallidus (GPe) (D2R-
650 SPNs or iSPNs) or to the Ep/GPi and SNpr (D1R-SPNs or dSPNs). Schemes have been
651 adapted from the mouse brain atlas [116].

652

653 **Figure 2: Identification of distinct domains of the rodent TS.**

654 (a) Schematic cartoon illustrating the TS. Double immunofluorescence of D2R (yellow) and
655 GFP (cyan) in the TS of *Drd2*-eGFP mice. D2R (cyan) immunolabeling in the rat and gerbil

656 TS. Note the presence in all these species of a longitudinal stripe adjacent to the GPe lacking
657 D2R-expressing SPNs. Scale bar, 200 μ m. **(b)** Cartoons and list of known markers allowing
658 the delineation of the D2R/A2aR-SPNs-lacking domain (in violet), and the two zones of the
659 D1R- and D2R/A2aR-SPNs-intermingled domain corresponding to the intermediate (in
660 orange) and lateral (in dark grey) parts of the tri-laminar zone [50]. Cx: Cortex; cc: corpus
661 callosum; GPe: external globus pallidus; AST: amygdalostriatal transition; CeA: central
662 amygdala, BLA: basolateral amygdala, LA: lateral amygdala; TS: tail of the striatum.
663 Schemes have been adapted from the mouse brain atlas [116].

664

665 **Figure 3: Distinct patterns of ERK phosphorylation within the mouse's TS domains.**

666 **(a)** Double immunofluorescence of pERK (yellow) and TH (cyan) in the TS of C57BL/6 mice
667 15 min after d-amphetamine (10 mg/kg) administration. Note that d-amphetamine-induced
668 ERK phosphorylation occurs preferentially in the D1R-SPNs of the D2R/A2aR-SPNs-lacking
669 domain. Scale bar, 200 μ m. High magnification of the area delineated by the white dashed
670 rectangle. Scale bar, 100 μ m. **(b)** Cartoons summarizing the distinct patterns of ERK
671 phosphorylation induced by a single injection of d-amphetamine (d-amph), MDMA, cocaine,
672 GBR12783 (DAT reuptake inhibitor), methylphenidate and PDE10A inhibitor (papaverine) in
673 the distinct mouse' TS domains. Note that papaverine increases preferentially pERK in D2R-
674 SPNs of the intermediate part of the D1R- and D2R/A2aR-SPNs-intermingled domain. Cx:
675 Cortex; cc: corpus callosum; GPe: external globus pallidus; AST: amygdalostriatal transition;
676 LA: lateral amygdala; TS: tail of the striatum. Schemes have been adapted from the mouse
677 brain atlas [116].

678

679 **Table 1. Markers with distinct expression in the medial, intermediate and lateral zones of the TS**

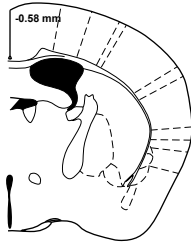
681	Markers	Zones/Domains	Species	References
682				
683	SP	medial-enriched	Mouse	[21,35,50]
684				
685	D1R	intermediate-poor	Mouse, Rat	[35,47]
686			<i>Drd1a-eGFP</i> mice	[35]
687			<i>Drd1a-tdTomato</i> mice	[47]
688				
689	TH	intermediate-poor	Mouse, Rat	[47,50]
690		medial-enriched	<i>Th-Cre:tdTomato</i> mice	[48](Allen Brain Atlas)
691				
692	CR	medial-enriched	Mouse, rat	[47,50]
693				
694	D2R	medial-poor	Mouse, Rat, Gerbil	[47]
695			<i>Drd2-eGFP</i> , <i>Drd2-Cre:RCE</i> mice	[35]
696			<i>Drd2-Cre:RCE</i> or <i>LacZ-TauGFP</i> mice	
697				
698	A2aR	medial-poor	Mouse, Rat, Gerbil	[47]
699			<i>Adora2a-Cre:YFP</i> mice	[35]
700				
701	PDE1b	medial-poor	<i>Pde1b-Cre</i> mice	[117](Gensat)
702				
703	Enk	medial-poor	Mouse	[47,50]
704			<i>Penk-2A-CreERT2:tdTomato</i> mice	[48](Allen Brain Atlas)
705			<i>PPE-eGFP</i> mice	[49]
706				
707	NT5E	medial-poor	Rat	[51]

708

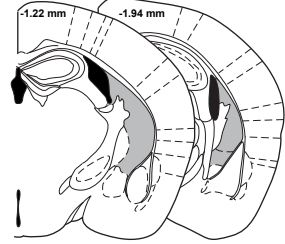
709 SP: Substance P; D1R: Dopamine D1 receptor; TH: Tyrosine hydroxylase; CR: Calretinin; D2R:
710 Dopamine D2 receptor; A2aR: Adenosine A2a receptor; PDE1b; Phosphodiesterase 1b; Enk;
711 Enkephalin; NT5E; Ecto-5'-nucleotidase

a *Mus musculus*

Caudal Striatum



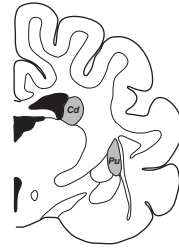
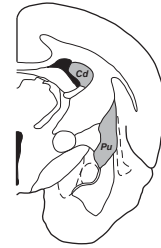
Tail of Striatum



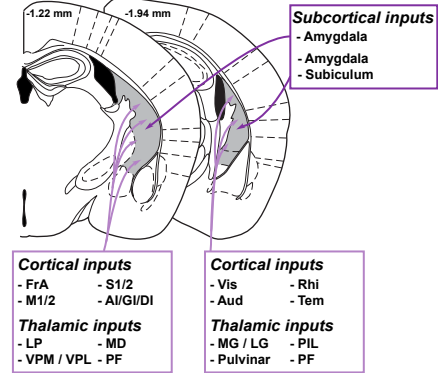
Tupaia belangeri

Felis catus

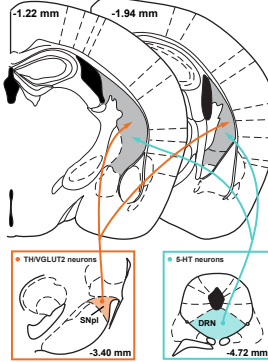
Macaca fascicularis



b Cortico-, Subcortico- and Thalamo-striatal inputs



c Monoaminergic inputs



c Outputs

